ORIGINAL ARTICLE

Photosynthesis measurements on the upper and lower side of the thallus of the foliose lichen *Nephroma arcticum* (L.) Torss

Konstantin Chekanov[1,2] · Elena Lobakova[1]

Abstract
The measurements of chlorophyll fluorescence play an important role in studies of lichen physiology. Usually, for foliose lichens fluorescence kinetics is recorded from the upper thalline side often exhibiting green color reflecting the presence of photosynthetic pigments. The lower side of such lichens is grey, dark-brown or black. At the first time, we evaluated photosynthetic activity distribution by chlorophyll fluorescence analysis on both lower and upper thallus sides for the foliose lichen *Nephroma arcticum*. We have demonstrated that photosynthesis proceeds not only on the green-colored upper side, but also on the gray lower side of the curled growing edges of the thallus lobes. These sides were differed in terms of PSII photochemical quantum yield, activity of non-regulatory dissipation and non-photochemical quenching of excited chlorophyll states (NPQ). Upper side was characterized by higher maximal PSII efficiency, whereas the lower one of the curled edges was characterized by higher actual photochemical quantum yield during actinic light acclimation. NPQ was higher on the upper surface, whereas, on the lower side (of the curled edges) non-regulatory dissipation was predominant. In terms of photosynthetic activity measurements, these results show, that actinic and measuring light reached the layer of phycobiont despite its shielding by mycobiont hyphae. On the melanized lower side in the basal thalline zone attached to the substratum photosynthesis was not detected. Lower side demonstrated higher level of light scattering in the reflectance spectra. We believe that different photoprotective mechanisms against high light are crucial on the upper and lower sides: NPQ on the upper surface, and light scattering and shielding by mycobiont on the lower side. Possible biological role of photosynthesis on the lower side is discussed.

Abbreviations

a. u.	Arbitrary units of chlorophyll fluorescence intensity
BRI	Browning reflectance index
CF	Chlorophyll fluorescence
ETC	Electron transport chain
F_J	The value of CF intensity at inflection J
Fm	Peak value of the CF intensity
Fo	Fluorescence intensity in the origin point of the curve
Fv	Variable fluorescence
Mo	Normalized initial slope of OJIP curve
$N(Q_A)$	Q_A turnover number
NDVI	Normalized Difference Vegetation Index
PAR	Photosynthetic active radiation
PS II	Photosystem II
Q_A	Primary PS II quinone acceptor
PRI	Photochemical Reflectance Index
R_{Red}, R_{NIR}	Total reflectance in the red and near infrared bands of the spectrum, respectively
$R(\lambda)$	Reflectance at the wavelength λ
RC	Reaction center
Sm, Ss	Normalized area between the OJIP curve and the horizontal line $F(t) = Fm$ in the case of multiple and single Q_A turnover number, respectively

✉ Konstantin Chekanov
chekanov@mail.bio.msu.ru

1 Department of Bioengineering, Faculty of Biology, Lomonosov Moscow State University, 1/12, Moscow, Russia 119234

2 Centre for Humanities Research and Technology, National Research Nuclear University MEPhi, Kashirskoe highway, 31, Moscow, Russia 115409

SR	Simple ratio
V_J	Relative height of O-J-step of OJIP curve
φ_{Do}	Quantum yield of thermal dissipation
φ_{Eo}	Quantum yield of electron transport
φ_{Po}	Maximal photosystem II (PSII) photochemical quantum yield of the dark-adapted thalli
Ψ_0	The probability of electron transport beyond Q_A

Introduction

Lichens are complex symbiotic systems with fungal structure-forming component (mycobiont), and algal component (photobiont). In some cases, they exhibit two algal components, cyanobiont and phycobiont, representing by diazotrophic cyanobacteria and green algae, respectively (Ahmadjian and Jacobs 1981; Stocker-Wörgötter 2001; Honegger 2012). Lichens are widely used as model organisms in physiological studies and as bioindicators in ecology. Estimating of parameters of primary photosynthesis based on the analysis of chlorophyll fluorescence (CF) induction kinetics (including parameters of 'fast' and stationary phases of inductive curves) is extensively applied in lichen biology in order to access the physiological state of these supraorganismal systems (Lange et al. 2001; Kalaji et al. 2016; Barták 2014; Stirbet et al. 2014; Goltsev et al. 2016; Palharini et al. 2020; Kuusinen et al. 2020). These parameters largely depend on the environmental conditions, embracing the presenceof pollutants and physiological conditions (Kalaji et al. 2016).

Nephroma arcticum (L.) Torss. (Nephromaceae, Peltigerales), also known as arctic kidney lichen, is a foliose lichen widely distributed in polar and subpolar regions (Urbanavichyus 2011; Thomson 1972; Rikkinen 2015). The phycobiont of *N. arcticum* is represented by the chlorophyte *Coccomyxa* (Chlorophyceae, Chlorococcales) (Büdel and Scheidegger 2008; Honegger 2012). This component is essential for inorganic carbon assimilation (Barták 2014). It is placed in the algal layer under the upper cortex of the thallus (Honegger 2012). Flat foliose thallus of *N. arcticum* is divided into lobes. It exhibits heteromerous structure (i.e., dorsoventral organization with distinct upper and lower sides/surfaces) (Büdel and Scheidegger 2008). One can distinguish two zones (parts) in this thallus. The first zone is the curled edge of the lobes up to 3 cm long unattached to the substratum. In accordance with commonly accepted lichenological terminology, it includes pseudo meristematic apical zone (lower than 1 mm long), subapical elongation zone (several millimeters long) and fully differentiated young part of the thallus (Honegger 2008). The second zone is the basal completely differentiated thalline area. It is attached to the substratum. Lower surface of the thallus in this zone is covered by rhizinae. In the present study, we specially focus on the photosynthetic features and assess its activity in various parts of thallus. We aimed to evaluate the distribution of *N. arcticum* phycobiont photosynthetic activity.

Metabolic processes, as well as its cell cycle are strictly controlled by the mycobiont (Stocker-Wörgötter 2001; Honegger 2012). The microalgae are essential for the lichen morphogenesis and survival (Stocker-Wörgötter 2001; Honegger 2012). On the one hand, the assimilation efficiency depends on intrathalline CO_2 availability which is affected by hydration status of the thallus (Lange et al. 2006 1999). These data may be obtained from the experiments of CO_2 exchange measurements as a function of lichen water potential (Lange et al. 2001). On the other hand, it depends on the primary processes of photosynthesis. They include absorption of light energy by photosynthetic pigments, its transfer to the reaction centers (RC) of photosystems, charge separation in the RC, electron transfer in the photosynthetic electron transport chain (ETC), production of NADPH for inorganic carbon reduction and conservation of the energy in the form of transmembrane proton gradient (Kalaji et al. 2016; Stirbet et al. 2014; Goltsev et al. 2016).

Photosynthetic activity of algal cells in the lichen is directly controlled by the mycobiont (Honegger 2012; Barták 2014). It varies in different thalline parts reflecting its growth patterns, energy demands, and anatomical features (Barták 2014). Generally, lichen thallus is characterized by a longitudinal and lateral heterogeneity of photosynthetic pigment content and photosynthetic activity (Conti et al. 2014; Wu et al. 2014; Barták et al. 2000; Hájek et al. 2016). As in heteromerous foliose lichen both these types have to be inherent in *N. arcticum*. This heterogeneity reflects the type of thallus growth (Büdel and Scheidegger 2008; Stocker-Wörgötter 2001). As it was shown for the foliose lichen *Peltigera aphthosa* (L.) Willd., parts of its thallus differed in the shape of the CF transient curves reflecting the efficiency of primary photochemistry (Maksimov et al. 2014; Chekanov et al. 2017). In foliose lichen *Flavoparmelia caperata* (L.) Hale, the efficiency of primary photochemistry in the marginal spots was higher than in the central ones (Baruffo et al. 2008). Noteworthy data about photosynthetic activity distribution were obtained using CF images technique (Jensen and Siebke 1997; Barták 2014). Fruticose lichens *Stereocaulon vesuvianum* Pers. and *Usnea antarctica* Du Rietz were characterized by intrathalline variation of photosynthetic activity which was high in all thallus except its subapical zone (for *S. vesuvianum*) and in the medial and the subapical zones (for *U. antarctica*) (Conti et al. 2014). In foliose *Xanthoria elegans* (Link) Th. Fr., the highest photosynthetic activity was observed in the central part of the thallus; then, during gradual senescence of the central part, the regions of high photosynthetic activity form ring-like zones (Barták et al. 2005). A decrease in the water potential of the

thallus caused by desiccation (Barták et al. 2000 2005) or increase of sucrose concentration (Hájek et al. 2006) was accompanied by the downregulation of its photosynthetic activity. The lichens with heteromeric thalline structure were characterized by the presence of a longitudinal heterogeneity of CF parameters. Photosynthetic activity was gradually reduced in the longitudinal direction ('photosynthetic gradient'), whereas there was no photosynthetic gradient in the homomeric thallus (Wu et al. 2014). However, in the thallus with gomeomeric structure, there is no photosynthetic gradient phenomenon (Wu et al. 2014).

Collectively, *N. arcticum* thallus is characterized by pronounced lateral and longitudinal heterogeneity. Therefore, it would be expected that various zones of its thallus should be characterized by a difference in parameters of photosynthetic activity and light absorbance by the phycobiont. We hypothesize the responses of primary photosynthesis of phycobiont to the light incident to the surface of the thallus would vary. We expected that the differences in their response would be due to variations in optical properties and anatomical organization. In this work, we try to test this conjecture. Toward this end we try to excite CF and follow phycobiont response on light fallen onto the lichen in different thallus zones. It should be noted that previous studies of the foliose lichen photosynthesis were performed only on the upper side of the thallus. In our study we also consider the case of light falling on the lower side.

Materials and methods

Lichen material collection

Nephroma arcticum (Peltigerales, Nephromaceae) thalli were collected in the vicinity of NA Pertsov White Sea Biological Station of Moscow State University, WSBS MSU (Kindo peninsula, Karelia, Russia, 66°34′ N; 33°08′ E). The lichens were collected in August of 2017 in the morning (10–12 a.m.). Sampled thalli grew in the forest shaded by trees on stones and soil surrounded or partially obscured by bryophytes and fallen leaves. The daylight photon flux density was in the range of 10–170 µmol of photosynthetic active radiation (PAR) quanta m^{-2} s^{-1} (as measured by a LiCor 850 quantum sensor [LiCor, Lincoln, NE, USA]), which are representative values for the forest near WSBS MSU in this time of the year (Chekanov et al. 2017). The measurements were conducted when the weather was sunny or cloudy. The data on climate parameters for a specified period of time are available at WSBS MSU site (http://www.wsbs-msu.ru/doc/view.php?ID=23). The relative air humidity was in the range of 55–65%. The temperature was in the range of 15–23 °C. Rounded hydrated thalli ca 150–250 cm^2 in area were selected. All procedures were performed with fresh hydrated thalli immediately after the collection. For CF measurements thalli were dark-adapted for 10 min, which is generally recognized as a sufficient time to 'open' all RCs of PSII (Kalaji et al. 2014).

The thallus cross-sections were examined using a Nikon SMZ745T stereomicroscope (Nikon, Japan) with a white LED Nikon C-FiD and photocamera MMC-31C12-M and Leica M165C motorized photomicroscope (Leica Microsystems, Germany) with white LED Leica CLS 150X and photocamera Leica DFC420 (5.0MP). Semi-thin cross-sections (10–15 µm thickness) in a plane perpendicular to the upper and lower thalline surfaces were prepared using a razor.

Reflectance spectroscopy

Reflectance spectra in the NIR and visible range were recorded on the lower and upper sides of *N. arcticum* thallus in the zone of curled edges and in the basal zone using an Agilent Cary-series UV–Vis (Agilent Technologies, USA) equipped with a 150 mm integrating sphere (Hitachi, Japan) located between the detector and the sample. Reflectance and transmittance spectra were recorded against the $BaSO_4$ standard (Hitachi, Japan). All measurements were done immediately after collection of fresh hydrated thalli. Fragments of lichen thallus were placed perpendicularly to the light source. The reflectance (R) in the red (at 650 nm) and NIR (at 800 nm) were taken for calculation of the standard Normalized Difference Vegetation Index (NDVI) (Peñuelas and Filella 1998),

$$NDVI = \frac{R(800 \text{ nm}) - R(650 \text{ nm})}{R(800 \text{ nm}) + R(650 \text{ nm})},$$

and the Simple Ratio (*SR*) (Peñuelas and Filella 1998),

$$SR = \frac{R(800 \text{ nm})}{R(650 \text{ nm})}.$$

To assume melanin content in the thalli, the browning reflectance index (BRI) (Chivkunova et al. 2001) was calculated as

$$BRI = \left(\frac{1}{R(550 \text{ nm})} - \frac{1}{R(700 \text{ nm})} \right) \times \frac{1}{R(750 \text{ nm})}.$$

CF transient analysis

Measurements of *N. arcticum* CF were performed in the field. Rapid CF transients, OJIP curves (Fig. 1A–C) (Strasser et al. 2004; Lazár 2006), were recorded with a Fluorpen FP100s PAM-fluorometer (PSI, Drasov, Czech Republic) after 10-min dark adaptation. Photon flux densities of the measuring and the saturating light were of 5 and of 3,000 µmol quanta m^{-2} s^{-1}, respectively. CF was excited by
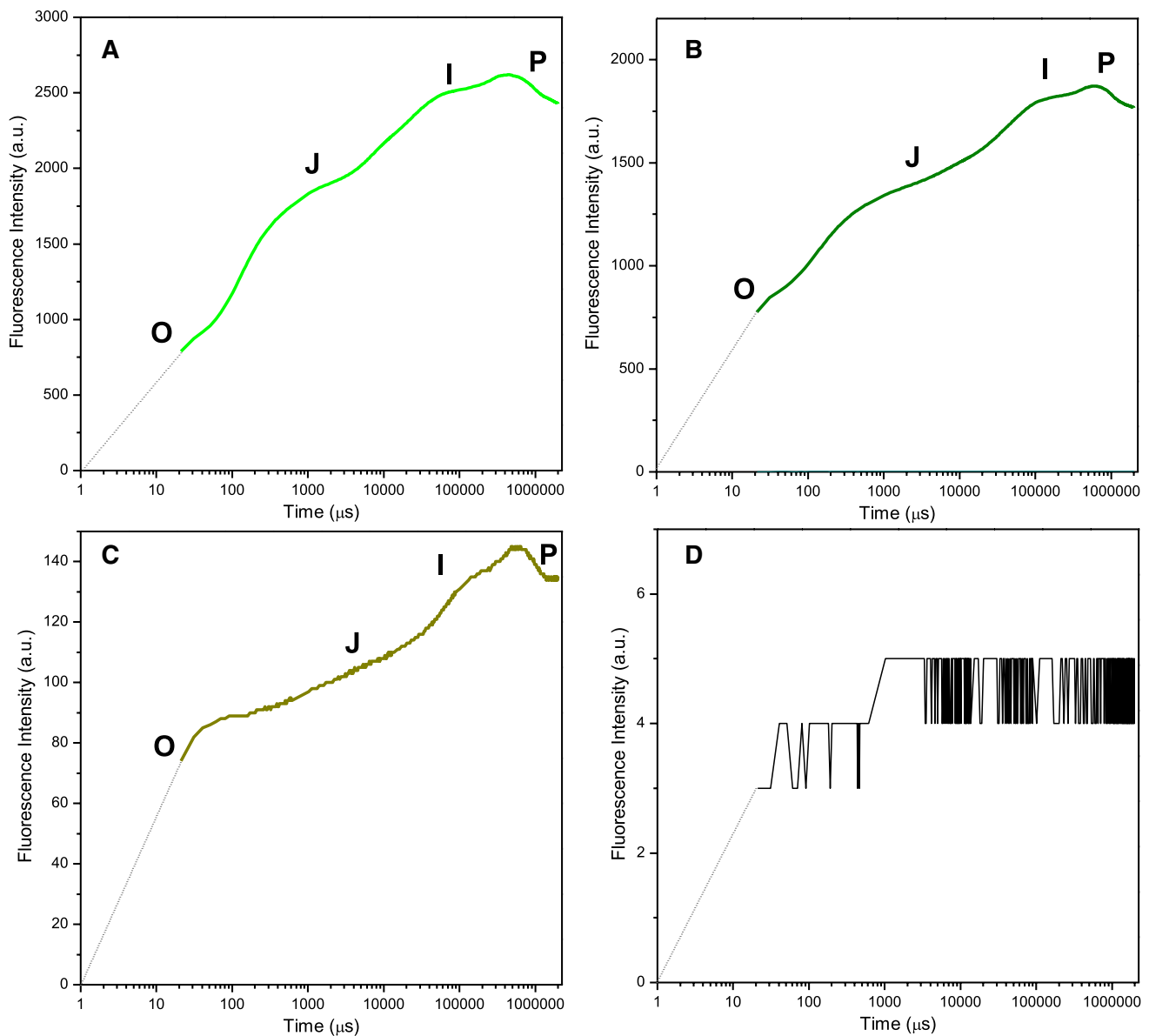
Fig. 1 Representative chlorophyll fluorescence transient curves (OJIP-curves) obtained on the upper side in the curled edges (**A**) and the basal (**B**) zones and on the lower side in the curled edges (**C**) and (**D**) basal zones of *Nephroma arcticum* thalli in the dark-adapted state. Characteristic points of the curves (O, origin, P, peak, as well as inflections J and I) are shown on panels A, B and C

a light-emitting diode ($\lambda = 455 \pm 5$ nm) and detected within the range of 697–750 nm. Optical aperture diameter was of 5 mm. The fragments of the thallus were tightly held between leaf clip and optical window. CF was registered in the cephalodia-free thallus zones.

The parameters of photosystem II (PSII) primary photochemistry were estimated based on the values of the CF intensity in the characteristic points of the OJIP curves (Fig. 1A–C; Strasser et al. 2004): the origin of the curve (Fo), the peak value of the CF intensity (Fm), the value of CF intensity at the inflection J (F_J), and the

variable fluorescence (Fv ≡ Fm − Fo). The maximal photosystem II (PSII) photochemical quantum yield of the dark-adapted thalli (φ_{Po}), the probability of electron transport beyond Q_A (Ψ_0), the quantum yield of electron transport (φ_{Eo}) and thermal dissipation (φ_{Do}) as well as the PSII primary quinone acceptor (Q_A) turnover number ($N(Q_A)$) we calculated automatically by a Fluorpen FP100s protocol.

The parameter Ψ_0 was calculated based on the value of relative O-J step height, $V_J = (F_J\text{-Fo})/\text{Fv}$:

$$\Psi_0 = 1 - V_J = \frac{Fm - F_J}{Fv}.$$

Quantum yields φ_{Po}, φ_{Do} and φ_{Eo} were estimated as

$$\varphi_{Po} = \frac{Fm - Fo}{Fm},$$

$$\varphi_{Do} = 1 - \varphi_{Po} = \frac{Fo}{Fm}$$

and

$$\varphi_{Eo} = \varphi_{Po} \times \Psi_0,$$

respectively.

We calculated two additional parameters of the OJIP curves, the normalized area between the OJIP curve and the horizontal line $F(t) = Fm$ ('area above the curve', Sm) and its normalized initial slope (Mo) in order to estimate $N(Q_A)$. Sm was calculated as

$$Sm = \frac{1}{Fv} \int_{25\ \mu s}^{t_m} (Fm - F(\tau)) d\tau,$$

where t_m is the time of the peak CF intensity. It was proportional to the energy consumed for multiple Q_A turnover (multiple events of Q_A oxidation and reduction during the time of CF intensity increasing from Fo to Fm). The initial slope (Strasser et al. 2004) was calculated as

$$Mo = \frac{1}{Fv} \left(\frac{dF}{dt} \right)_{t=25\ \mu s} \approx \frac{F(300\ \mu s) - F(50\ \mu s)}{250\ \mu s \times Fv},$$

where $F(t)$ is fluorescence intensity at time t. Thus, assuming initial rise of OJIP curve is exponential (Strasser and Stirbet 2001; Strasser et al. 2004), normalized area above the curve in the case of single turnover, Ss, can be calculated as

$$Ss = \frac{V_J}{Mo}.$$

Thus, Q_A turnover number, the number of Q_A oxidation/reduction events at tome of CF rising from Fo to Fm, is

$$N(Q_A) = \frac{Sm}{Ss}.$$

Stationary fluorescence analysis

Stationary CF was registered with a Fluorpen FP100s PAM-fluorometer in the field (see previous subsection). To induce the processes of regulatory non-photochemical quenching of the excited chlorophyll states, dark-adapted cells were exposed to actinic light of high photon flux density ($\lambda = 455 \pm 5$ nm, 800 µmol quanta m^{-2} s^{-1}), saturation pulse

was applied each 12 s during acclimation to actinic light for detection of maximal CF intensity in the light-adapted state (Fm′). The parameters of measuring and saturating light were as in the previous subsection. Before actinic light exposure, Fo and Fm values were registered. There were a total of 5 flashes of saturation light during actinic light illumination. Other parameters were as in the previous section. The Stern–Volmer non-photochemical quenching parameter (Demming-Adams and Adams 1992) was calculated as

$$NPQ = \frac{Fm}{Fm'} - 1.$$

Quantum yields of regulatory, $\varphi(NPQ)$, and non-regulatory, $\varphi(NO)$, energy dissipation, as well as actual photochemical quantum yield φ_P, were calculated as

$$\varphi(NO) = \frac{Ft}{Fm},$$

$$\varphi(NPQ) = \frac{Ft}{Fm} \times \frac{Fm - Fm'}{Fm'},$$

$$\varphi_P = \frac{Fm' - Ft}{Fm'},$$

where Ft is stationary CF intensity during illumination by the actinic light (Lazár 2015).

Statistical analysis

The data were collected on 15 fresh *N. arcticum* thalli immediately after their collection.

The obtained data were processed using the OriginPro 8 software (OriginLab Corporation, USA). The non-parametric statistical Main–Whitney standard *U*-test was used (Lazár 2006) to analyze the OJIP curves. The median values as well as 25th (p25th) and 75th (p75th) percentiles were presented.

For analysis of the reflectance spectra indices the data were tested for normality applying the standard Shapiro–Wilk criterion. Median values and their standard deviations are shown. The standard F-test was used to discriminate the datasets ($P = 0.95$).

Results

N. arcticum thallus morphology and anatomy

The morphology of the thalli (Fig. 2A) followed the classical *N. arcticum* description (Parr and Wilson 2014). The foliose thallus of the lichen was divided into several lobes 5–15 cm

Fig. 2 The thallus of *Nephroma artcticum*. The thallus in its natural habitat (scale bar: 5 cm) (**A**). General view of the thallus from the upper (scale bar: 2 cm) (**B**) and lower side (scale bar: 2 cm) (**C**). Thallus cross-section in the zone of curled edges (scale bar: 150 μm), (**D**) and in the basal zone (scale bar: 150 μm) (**E**); *Ph*—phycobiont, *Md*—medulla, *UCr*—upper cortex, *LCr*—lower cortex, *Rh*—rhizines
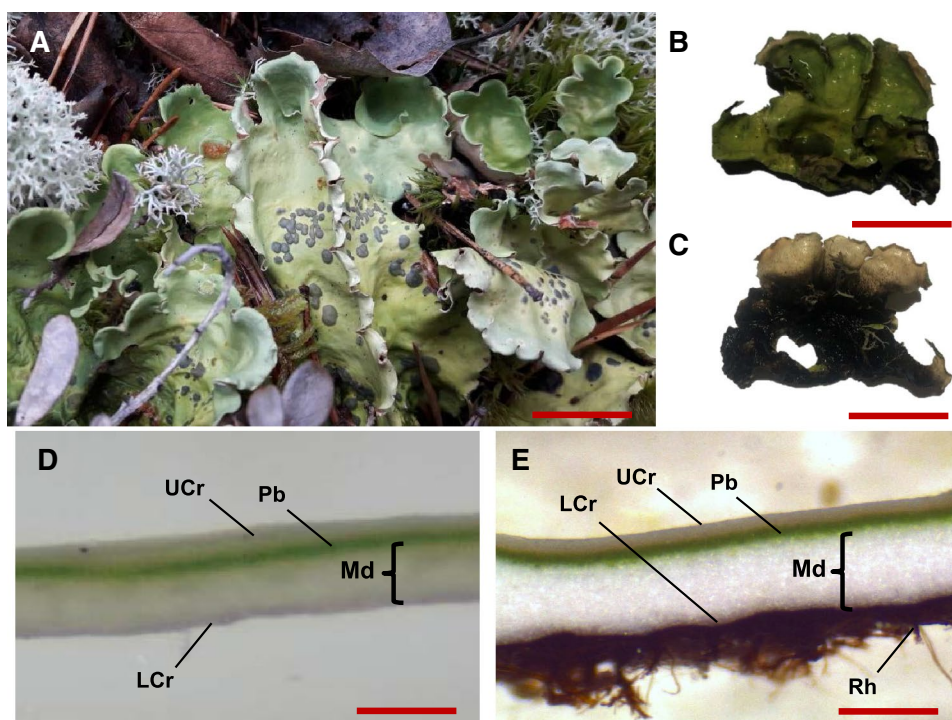
Table 1 Thickness of *N. arcticum* thallus layers on the cross-sections in curled edges and basal zone

Thallus zone	Curled edges (μm)	Basal zone (μm)
Upper cortex	10	15–20
Phycobiont layer	10	15–20
Medulla	50–60	80–100
Lower cortex	5–10	70–90

The ranges between maximal and minimal values from 15 fresh thalli are shown

length and up to 7 cm width. The growing edges of the lobes (0.5–1.5 cm length) were curled and raised (Fig. 2A). In the current work, we used two terms throughout the text for classification on the *N. arcticum* thallus zones: curled edges and basal zone.

The upper surface of the thallus was lime green, greenish or yellow-greenish with blue-green or dark-blue cephalodia (Fig. 2B). Except for the zone of curled edges, the lower thalline side was dark-brown or black (Fig. 2C).

Organization of stratified thallus structure on the cross-sections was similar in the completely differentiated part of curled edges (Fig. 2D) and in the basal zone (Fig. 2E). Upper and lower cortex, medulla and phycobiont layer were distinguished (Fig. 2D, E). Medullar layer formed by loosely interwoven aerial hyphae (plectenchyma) was localized under the layer of phycobiont. The layer of phycobiont was localized close to the upper side of the *N. arcticum* foliose thallus

under the upper cortex (or cortical layer) (Fig. 2D, E). The periphery of the thallus is surrounded by the relatively thin conglutinate peripheral cortex (Table 1). The layer of phycobiont was localized directly under the upper cortex. In the zone of curled edges upper and lower cortex, medulla and phycobiont layer were thinner (Table 1). The thallus was attached to the substratum by rhizines in the basal zone. In the zone of curled edges rhizines were absent.

Reflectance spectra

Upper surface of the *N. arcticum* thallus in the zone of curled edges and in the basal zone was characterized by reflectance spectra typical for photosynthetic plant tissues (Fig. 3A, B) with two minima corresponding to absorption bands in the red and blue-green region of the spectrum. Spectra recorded from the lower surface in the zone of curled edges (Fig. 3C) were characterized by monotonously increasing of the reflectance ($\forall \lambda: dR(\lambda)/d\lambda \geqslant 0$) indicating high contribution of light scattering to the spectral shape. At the same time, they exhibited inflections in the red and blue-green region revealing the presence of photosynthetic pigments. The lower black-colored surface of the basal zone of the *N. arcticum* thalli was characterized by the lowest reflectance level (Fig. 3D). In this case $R(\lambda)$ also monotonously increased, and the spectra did not possess pronounced inflections.

Visual analysis of the spectra was confirmed by spectral indices (Table 2). The values of NDVI and SR on the upper surface were relatively high and close to each other in the
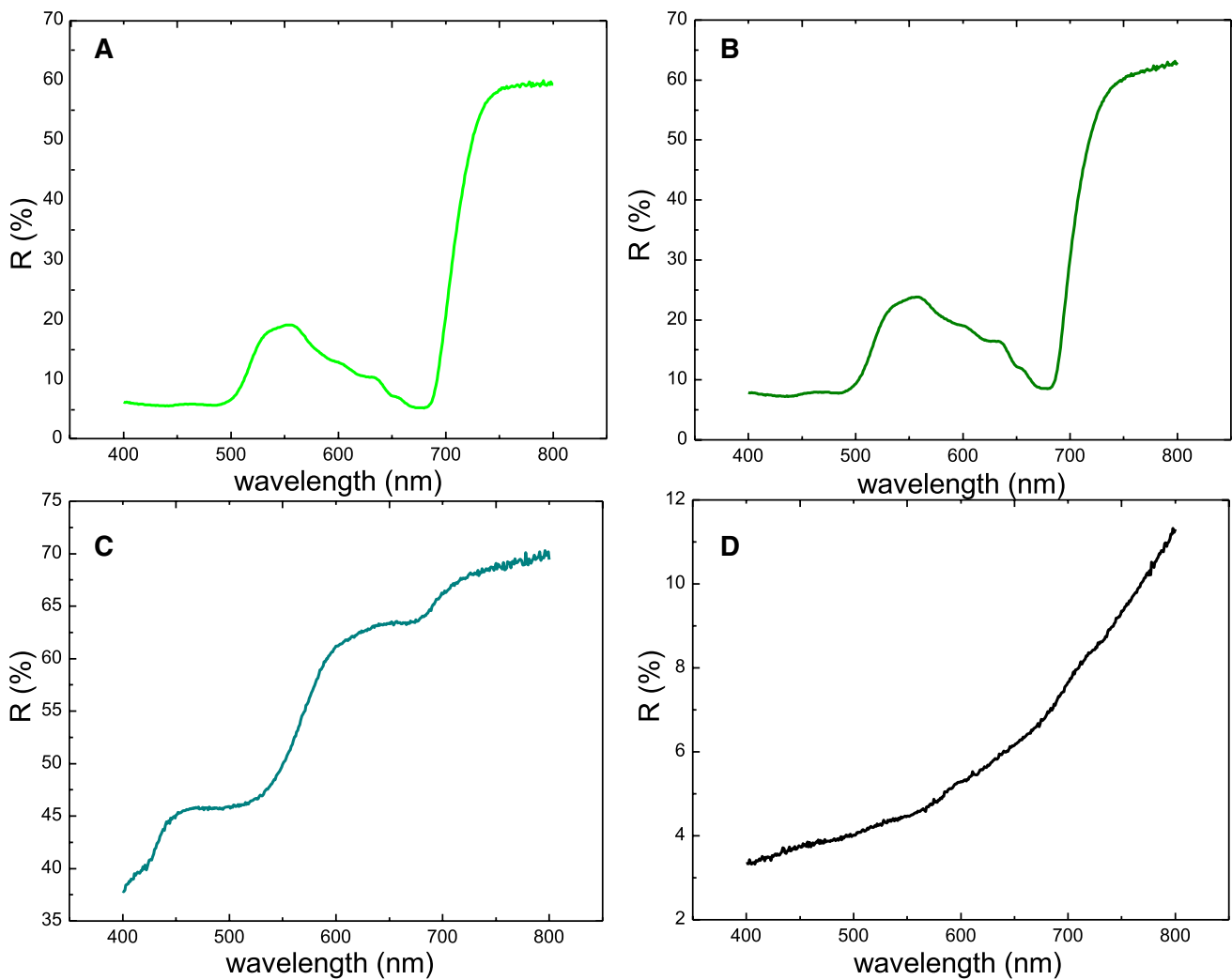
Fig. 3 Representative reflectance spectra of the *Nephroma arcticum* thallus on the upper surface of the thallus in the zone of curled edges (**A**), on the upper surface in the basal zone (**B**), on the lower surface in the zone of curled edges (**C**) and on the lower surface of the thallus in the basal zone (**D**)

Table 2 Spectral reflectance indices of different *Nephroma arcticum* thallus zones

Parameter	Basal zone		Curled edges	
	Upper	Lower	Upper	Lower
SR	2.50 ± 0.40^a	1.54 ± 0.25^b	2.82 ± 0.32^a	1.07 ± 0.10^c
NDVI	0.43 ± 0.08^a	$0.21 \pm 0.0.2^b$	0.48 ± 0.07^a	0.03 ± 0.02^c
BRI	2.46 ± 0.02^a	2.48 ± 0.40^a	0.70 ± 0.00^b	129.24 ± 3.6^c

Mean values ± standard deviations are shown. Same letters indicate statistically equal groups. The data were collected on 15 fresh *N. arcticum* thalli immediately after their collection

zone of curled edges (NDVI = 0.43 ± 0.07; SR = 2.50 ± 0.40) and in the basal zone (NDVI = 0.48 ± 0.07; SR = 2.82 ± 0.32) of the thallus suggesting high contribution of chlorophyll absorbance and low contribution of the light scattering (Table 2). On the lower surface of the zone of curled edges, both indices were significantly lower (NDVI = 0.21 ± 0.02; SR = 1.54 ± 0.25), and they were close to zero on the lower surface of the basal zone (NDVI = 0.03 ± 0.02; SR = 1.07 ± 0.10) (Table 2). The values of BRI on the upper side were similar in the zone of curled edges and the basal zone: their average values were 2.46 and 2.48, respectively. On the lower thalline side in the zone of curled edges, BRI was the lowest (0.76). On the lower side in the basal zone, values of the index were significantly higher, than in all other cases (129.24 in average) (Table 2).

CF transient analysis

The representative OJIP curves (i.e., characterized by main shape parameters closed to median for a zone of the thallus) recorded from the lower and upper sides of *N. arcticum* foliose thallus in the zone of curled adges and in the basal zone are shown at Fig. 1. They were characterized by two inflections, J (approximately at 2 ms) and I (approximately at 30 ms) and monotonous increasing of the CF intensity from the initial point O to the maximum P during illumination of the thallus by saturating pulse. After the point P, CF intensity decreased (Fig. 1A–C). The parameters of the OJIP curves were calculated as described in Methods are shown in Table 3. The highest values of CF intensity in the initial point of the curves (Fo) were detected on the upper side of the zone of curled adges and in the basal zone (972 a.u. and 939 a.u., respectively). Fo was of 58 a.u on the lower side of the zone of curled adges. On the lower side of the basal zone, the lowest Fo values (5 a.u.) were observed. The values of φ_{Po} were approximately the same on the upper side of the basal zone and the zone of curled edges—their median value was of 0.59 in both cases. φ_{Po} was of 0.43 on the lower side of the zone of curled edges (Table 3). All thalline regions, except the lower side of the basal zone, had relatively high Ψ_0 values (0.40, 0.34 and 0.49 for the upper side of the basal

zone and the zone of curled edges as well as the lower side of the zone of curled edges, respectively). It should be noted that Ψ_0 of the lowest side of the zone of curled edges was the highest, despite a relatively low φ_{Po} value (Table 3). Collectively, all the areas of the thallus under scrutiny, except the lower side of the basal zone, were characterized by approximately equal values of φ_{Eo} (0.24 on the upper surface of the basal zone and 0.21 on both sides of the zone of curled edges) (Table 3). Median values of $N(Q_A)$ were the highest on the upper side of the basal zone ($N(Q_A) = 2199$). In the zone of curled edges, the parameter was as high as 1795 and 1773 on the upper and lower side, respectively (Table 3). The difference in $N(Q_A)$ values in all thalline zones, except the lower surface of the basal zone, however, was statistically insignificant.

The shape of the OJIP curves obtained on the lower side of the basal zone differed from the others (Fig. 1D). It lacked typical pronounced features of CF transient. Formal calculation of OJIP curves parameters gave following median values: $N(Q_A) = 8$, $\Psi_0 = 0.25$, $\varphi_{Po} = 0.33$, $\varphi_{Eo} = 0.10$ (Table 3).

Stationary CF analysis

Stationary phase of the CF induction curves was registered in the zone of curled edges (Fig. 4A) and the basal zone (Fig. 4B) on the upper surface of the thallus, and on the lower surface of the zone of curled edges (Fig. 4C). Overall, fluorescent signal was higher on the upper surface. There, a pronounce CF quenching was observed after the actinic light exposure.

Actinic light exposure led to the decrease of the PS II photochemical quantum yield. On the upper surface the values of φ_P were lower than 0.14 after 40 s of measurement, whereas on the lower surface of the zone of curled edges φ_P values were as high as 0.30 (Fig. 4D).

During observation time the quantum yield of regulatory dissipation reached its stationary values (Fig. 4E). On the upper surface the $\varphi(NPQ)$ values were higher as that on the lower one (0.68–081 vs 0.18–0.19). On the upper thallus surface, the quantum yield of non-regulatory dissipation gradually decreased during the actinic light illumination (to 0.15) (Fig. 4F). At the same time, on the lower surface $\varphi(NO)$ was retained relatively stable and higher than that on the upper surface (in the range of 0.56–0.58) (Fig. 4F). The Stern–Volmer NPQ parameter increased gradually on the upper surface of the *N. arcticum* thalli (up to 5.40), whereas it was low and relatively constant on the lower surface in the zone of curled edges (0.02–0.05) (Fig. 4G).

Table 3 The characteristic parameters of the OJIP curves and primary photochemistry indexes obtained from their shape in different *Nephroma arcticum* thallus zones

Parameter	Basal zone		Curled edges	
	Upper	Lower	Upper	Lower
Fo, a.u	939[a]	5[c]	972[a]	58[b]
	829–1068	6–7	873–1027	56–63
Fm, a.u	1872[a]	9[c]	2615[a]	105[b]
	1657–2827	7–12	1798–2881	74–122
Fv, a.u	1120[a]	3[c]	1666[a]	48[b]
	928–1802	2–4	795–1849	19–61
$N(Q_A)$	2199[a]	8[c]	1795[a]	1773[a]
	1881–2604	3–11	1403–2472	947–2123
Ψ_0	0.40[a]	0.25[b]	0.34[a]	0.49[a]
	0.33–0.42	0.00–0.33	0.26–0.36	0.40–0.57
φ_{Po}	0.59[a]	0.33[c]	0.59[a]	0.43[b]
	0.58–0.61	0.27–0.36	0.44–0.66	0.24–0.50
φ_{Eo}	0.24[a]	0.10[b]	0.21[a]	0.21[a]
	0.20–0.26	0.00–0.13	0.10–0.23	0.10–0.29
φ_{Do}	0.41[a]	0.67[c]	0.41[a]	0.57[b]
	0.39–0.43	0.64–0.71	0.34–0.57	0.51–0.78

Median values and the range between 1st and 3rd quartiles are shown. Same letters indicate statistically equal groups of data. The data were collected on 15 fresh *N. arcticum* thalli immediately after their collection
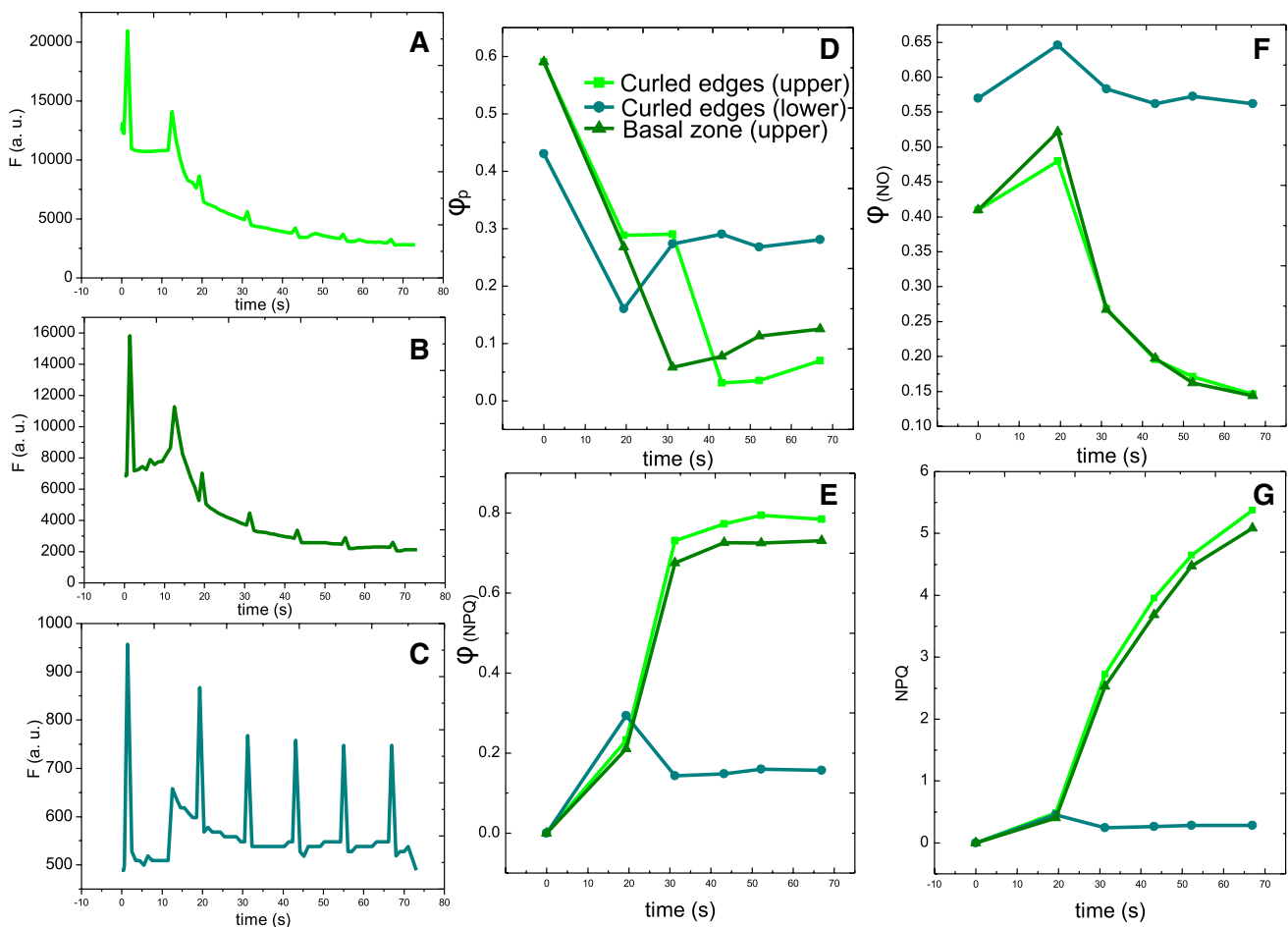
Fig. 4 Chlorophyll fluorescence parameters of the *Nephroma arcticum* during acclimation to the actinic light. Chlorophyll fluorescence induction curves detected on the upper surface of the thallus in the zone of curled edges (**A**), on the upper surface in the basal zone (**B**), on the lower surface in the zone of curled edges (**C**). Photochemical quantum yield of PS(II) (**D**). Non-regulative dissipation quantum yield (**E**). Regulative dissipation quantum yield (**F**). The Stern–Volmer NPQ parameter (**G**)

Discussion

The upper side of the thallus was green-colored indicating a high chlorophyll content, whereas the lower side of the zone of curled edges was grey suggesting its low content. Visual observation of the thalli was confirmed by the analysis of the absorbance spectra. High NDVI and *SR* values on the upper surface of the thallus indicated potentially high level of light absorbance by chlorophylls (Peñuelas and Filella 1998; Gloser and Gloser 2007). In the foliose lichen *Umbilicaria hirsuta* (Sw. ex Westr.) Hoffm., NDVI ranges from 0.3 to 0.5 depending on its hydration (Gloser and Gloser 2007). *Ramalina lacera* (With.) J. R. Laundon as a rule is characterized by NDVI is in the range 0.32–0.38 (Garty et al. 2000). On the upper surface of physiologically active *P. aphthosa* in the wet state it is c.a. 0.50 ± 0.04 (Bokhorst et al. 2012). *N. arcticum* upper thallus surface in the wet state was characterized by a similar NDVI. These values fell into the range of average landscape values in Polar latitudes during vegetation (Raynolds et al. 2013; Sotille et al. 2020) and specifically into the range typical for surfaces covered by lichens (Gamon et al. 2013). NDVI values strongly depend on physiological status of the thallus, e.g., on its hydration (Gloser and Gloser 2007; Sotille et al. 2020). Low dispersion of NDVI values obtained in the work suggested relative uniformity of lichen material. On the lower surface of the basal zone, low values of the spectral indices reflected low ability of light absorption and utilization. On the lower surface of the *N. arcticum* thallus in the zone of curled edges NDVI was moderately low, whereas in the basal-brown-colored zone on the lower side the index was close to zero. It might reflect the difference in photosynthetic capacity in different zones on the thallus. The data on NDVI measurements for foliose lichens are poor. Previously, the difference in NDVI between the upper and curled lower surface of the thallus was reported in foliose *P. aphthosa* (Bokhorst et al. 2012).

Similar situation was observed: lower surface was characterized by lower NDVI surface than upper. Strong decrease of the reflectance in the dark-brown lower surface in the basal zone indicated signs of thallus melanization (McEvoy et al. 2007a; Mafole et al. 2017; Rassabina et al. 2020). Formally calculated indices values on the lower surface in this zone reflected inability to absorb the light by photosynthetic pigments. Based on the shape of the CF induction curves obtained there and the formal calculation of its parameters, photosynthesis was also absent in this zone, when light fell onto the lower surface.

Non-melanized thalli of the foliose lichens *Peltigera aphthosa* and *Peltigera membranacea* (Ach.) Nyl. inhabiting similar to *N. arcticum* ecological niches are characterized by average BRI values (measured on the upper side) in the range of 2.1–2.8 (Mafole et al. 2019a). In *Lobaria pulmonaria* L. (Hoffm.) it ranges from 2.1 to 4.1 depending on habitat (McEvoy et al. 2007a; Mafole et al. 2019a). In some dark-colored foliose lichens BRI of nonmelanized thalli are higher, e.g., in *Pseudocyphellaria gilva* (Ach.) Malme and *Sticta sublimbata* (J.Steiner) Swinscow & Krog BRI = 7.5 and BRI = 8.2, respectively (Mafole et al. 2019a). At the same time, in the grey-colored *Cetraria islandica* (L.) Ach. BRI is lower than one (Mafole et al. 2019a). Thus, on the upper surface of the *N. arcticum* thalli, BRI values were closer to that of foliose green-colored lichens from similar habitats. *BRI* on the grey-colored lower side in them zone of curled edges were similar to that of grey-colored *C. islandica*. Collectively, *BRI* indices in the above-mentioned zones of *N. arcticum* thallus indicated absence of pronounced melanization. At the same time, it was strong on the lower side of the basal zone based on high values of the parameter (Mafole et al. 2019a).

Melanization is a common feature of fungi. Fungal melanins are chemically diverse group of pigments characterizing by black or brown color disappearing after their oxidation, insolubility in hot water, acids and organic solvents (with some exceptions), and solubility in alkali (Butler and Day 1998; Gauslaa and Solhaug 2001; Gessler et al. 2014). There are following main types of fungal melanins: brown-to-black eumelanin (3,4-dihydroxyphenylalanine) and allomelanin (1,8-dihydroxynaphthalene melanin), yellow-to-red pheomelanins as well as pyomelanin (Plonka and Grabacka 2006; Gessler et al. 2014). It is commonly accepted that ascomycetes accumulate mainly allomelanin, whereas eumelanin is more typical for basidiomycetes (however, there are some exceptions, see below) (Ametrano et al. 2019). Chemical nature of melanins in different lichen genera is poorly studied. *Cetraria islandica* (L.) Ach. (Lecanorales) and *Pseudevernia furfuracea* (L.) Zopf. (Lecanorales) have allomelanin (Rassabina et al. 2020). *L. pulmonaria* (Peltigerales) seems to accumulate eumelanin (Matee et al.

2016). In the dissertation by Mafole (2017) it is speculated based on C/N ratio that lichens from the order Peltigerales accumulate eumelanin (based on the data obtained from *Leptogium furfuraceum* (Harm.) Sierk, *Lobaria retigera* (Bory) Trevis, *Pseudocyphellaria aurata* (Ach.) Vain., *Pseudocyphellaria gilva*). It was proposed, that accumulation of N-rich eumelanin in Pletigerales was conditioned by exhibiting of N-fixing cyanobacteria in their thallus (Matee et al. 2016; Mafole 2017; Mafole et al. 2019b). Summarizing, cyanobacteria-containing Peltigerales lichens accumulates eumelanines, whereas others accumulate mostly allomelanines (however, the latest statement should be verified) (Mafole et al. 2019b). Since, *Nephroma* is also a member of Peltigerales, it should also have eumelanin, but there are no detailed studies of this genus.

Melanization is an essential process in the lichen thallus and it exhibits high physiological value (McLean et al. 1998; Fortuna et al. 2017). Most likely, it also plays an important role in the protection of lichen thallus during its development (Gauslaa and Solhaug 2001). Collectively, melanin accumulation is considered as one of adaptation to adverse conditions (Gauslaa and Solhaug 2001; Gessler et al. 2014). They play a role in protection against extreme temperatures, irradiation, metal binding, maintaining of water regime, and others (Butler and Day 1998). Foliose lichens accumulate melanins either on the upper surface exposed to light or on the lower side mainly facing a substratum. On the upper side, they protect thallus against UV and visible light irradiation (McEvoy et al. 2007a; Mafole et al. 2017 2019a). Under high light, melanins serve as photoprotective compounds reducing negative effects of photoinhibition (Mafole et al. 2019a). At the same time, it facilitates downregulation of photosynthesis in terms of O_2 production, CO_2 assimilation, electron transport rate and PSII primary photochemistry under low light (Mafole et al. 2017). Most likely, these functions are not the case of *N. arcticum* growing in the forest and shaded by trees. *Nephroma* accumulates melanin in the lower cortex during thallus development (Mafole et al. 2019a), which was in accordance with our reflectance spectroscopy data. Being accumulated on the lower side of foliose lichen thalli melanin may play a role in adsorption of metal ions (Butler and Day 1998; Plonka and Grabacka 2006; Mafole et al. 2019b). It is important for neutralizing toxic metals and accumulation of necessary elements. Fungal melanins bind Al, Zn, Fe, Mg, Zn, K, Ca, Ba, Ni, V and Cu (Butler and Day 1998; Garty et al. 2000; Fortuna et al. 2017; Mafole et al. 2019b). The lichen *Trapelia involuta* (Taylor) Hertel accumulates U in its cell wall due to melanin presence (McLean et al. 1998). Melanin may also play a role in protection against parasitic microorganisms and soil nematodes (Plonka and Grabacka 2006).

On the upper side of the thallus, as well on the lower side of the zone of curled edges, typical CF induction curves

were recorded (Stirbet et al. 2014). Thus, electron transport in the chloroplast ETC was induced by illumination of *N. arcticum* in all these cases. In other words, actinic and saturating light reached the phycobiont layer despite its shielding by the mycobiont. In the case of measurements on the lower side in the basal zone, CF induction curves typical of active photosynthetic apparatus were not detected. Thus, the lower side of the basal zone did not possess a photosynthetic activity.

The values of φ_{Po} on the lower side of the zone of curled edges were lower than those in the upper side of the thallus. Consequently, it was characterized by a lower fraction of open PSII RC in the dark-adapted state. The latest zone, however, was characterized by large Ψ_0 values. It indicated a low level of ETC overreduction. Most likely, RC absorbed low amounts of light energy in this zone, due to optic shielding by the mycobiont (Valladares et al. 1996) and the light scattering by the cortex (Barták et al. 2015). Thus, in the case of photosynthesis induction by light fallen onto lower surface of this zone the ETC was characterized by a lower level of PSII excitation pressure. As a result, in all photosynthetically active zones of the thallus, approximately the same values of φ_{Eo} were observed, i.e., the effectiveness of the electron transport beyond PSII RC remains the same. The turnover of the primary quinone acceptor PSII was also equally effective. These results were obtained in the case of measurements on both lower and upper side in the zone of curled edges.

High light exposure leads to excessive energy absorption and excited chlorophyll states accumulation in the phototrophic cell. It results in the increase of the risk of reactive oxygen species overproduction and photodamage (Demmig-Adams and Adams 1992; Lazár 2006; Kalaji et al. 2016; Goltsev et al. 2016). During illumination of the *N. arcticum* thallus by the actinic light on its upper surface the phycobiont built up the mechanisms of regulatory non-photochemical quenching of the excited chlorophyll states. The machinery of non-photochemical quenching plays an important role in decreasing the risk of photodamage of the PSII core (Demmig-Adams and Adams 1992; Lazár 2006; Kalaji et al. 2016). It also resulted in the non-regulatory quenching decline, since it grouped the processes competitive to the regulatory quenching. Because the cell cannot utilize all absorbed energy under high light, it is also important to decrease the yield of primary photochemistry (Lazár 2006; Goltsev et al. 2016). It resulted in the φ_P decline in the case of measurements on the upper thallus surface. Illumination of the zone of curled edges on the lower surface did not lead to regulatory quenching upregulation. Moreover, primary photochemistry decline was less pronounced. Position of phycobiont in a lichen is optimal for light absorbance; close proximity to plectenchyma of

medulla provides necessary gas exchange (Büdel and Scheidegger 2008; Honegger 2012). Being localized closer to the upper side of the *N. arcticum* foliose thallus, the phycobiont layer is exposed to the solar irradiation. At the same time, a massive medulla layer and lower cortex shielded it on the lower side. Thickness of these layers was lower in the zone of curled edges. Moreover, in this zone the thallus lacked melanization and did not exhibit rhizines. It made it possible to absorb the light falling onto the lower side in this zone by photosynthetic pigments. At the same time, mycobiont protects algal cells against excessive irradiation. It produce protective colorless compounds, such as atranorin, effectively absorbing UV (Rao and LeBlanc 1965). Crystals of such compounds reflect and scatter PAR that also contribute to attenuation of light received by the phycobiont (McEvoy et al. 2007b; Solhaug et al. 2010). Cortical layers of *N. arcticum* contain usnic acid, absorbing significant amount of UV, whereas nephroarctin and phenarctin deposited mainly in the medulla effectively absorb UV-B (McEvoy et al. 2007b). At the same time, crystals of usnic acid and other secondary metabolites scatter and reflect radiation from the visible range (McEvoy et al. 2007b). Taking into account the high level of light scattering on the lower side of the thallus and low CF signal in the zone of curled edges, it might also contribute to photoprotection of phototrophic cells. Phycobiont cells were also shielded by the mycobiont layer from excessive light irradiation. The decrease intensity of the actinic light affected phycobiont cells that gave the possibility to retain relatively high values of the photochemical yield under high light. Collectively, the data suggest that in the case of the upper side of the *N. arcticum* thallus photoprotection of the phycobiont cells was realized by their own active mechanisms, such as non-photochemical quenching, whereas in the case of the lower side the mycobiont played main role in the protection by optic shielding and light scattering. On the lower side of the basal zone the thallus is black. Photosynthetic activity was not detected there. This black color also is typical to the lower edge of the subapical zone, where the lichen is attached to a substratum.

Selecting a thallus region is crucial for accurate CF measurements. To the best of our knowledge, most of the previous studies of photosynthetic activity in the foliose lichens thalli focused on their upper surface. Marginal part of *N. arcticum* is curled upward (Fig, 2a). In the *L. pulmonaria*. Taylor there are small areas of high photosynthetic activity. After pre-illuminating with bright light of the curling thalli, the areas of increased photosynthetic activity were larger than in a flat uncurled thallus due to self-shading. On the other hand, in flattened thalli, the retention of photosynthetic activity after the pre-illumination was not observed. Barták et al. (2006) suggested that curling of foliose lichens lobe is a photoprotective mechanism against photodamage during thallus desiccation. Thus,

thallus curling plays a major physiological role. Under drying conditions, curled thallus edges protect the areas under them by shading which reduces photodamage of desiccating algal phycobiont. In this case, the curled edges of the thallus are capable to absorb light and perform photosynthesis (Barták et al. 2006). Morphology of the thallus and photosynthetic activity distribution may also be important for *N. arcticum*. As a rule, in the forest, most part of the area of foliose lichen thallus is under a layer of mosses and fallen leaves; thallus also can be shielded by grass or other lichens (Kuusinen et al. 2020). In this case, the curled edges of the thallus can be its single part, able to absorb light.

Concluding, the studies of fresh *N. arcticum* thalli gives new information about the physiological role of different *N. arcticum* thallus patterns. Based on CF intensity analysis in native thalli, new data about distribution of photosynthetic activity distribution were obtained from the lower side of dorsoventral foliose thalli.

Author contributions KC—manuscript preparation; CF measurements; spectroscopy; data interpretation. EL—manuscript preparation; experiment design; project administration.

References

Ahmadjian V, Jacobs JB (1981) Relationship between fungus and alga in the lichen *Cladonia cristatella* Tuck. Nature 289.5794:169

Ametrano CG, Muggia L, Grube M (2019) Extremotolerant black fungi from rocks and lichens. In: Tiquia-Arashiro SM, Grube M (eds) Fungi in extreme environments: ecological role and biotechnological significance. Springer, Cham, pp 119–143

Barták M (2014) Lichen photosynthesis. Scaling from the cellular to the organism level. In: Hohmann-Marriott MF (ed) The structural basis of biological energy generation. Springer, New York, pp 379–400

Barták M, Hájek J, Gloser J (2000) Heterogeneity of chlorophyll fluorescence over thalli of several foliose macrolichens exposed to adverse environmental factors: interspecific differences as related to thallus hydration and high irradiance. Photosynthetica 38(4):531–537

Barták M, Gloser J, Hájek J (2005) Visualized photosynthetic characteristics of the lichen *Xanthoria elegans* related to daily courses of light, temperature and hydration: a field study from Galindez Island, maritime Antarctica. Lichenologist 37(5):433–443

Barták M, Solhaug KA, Vráblíková H, Gauslaa Y (2006) Curling during desiccation protects the foliose lichen *Lobaria pulmonaria* against photoinhibition. Oecologia 149(4):553–560

Barták M, Trnková K, Hansen ES, Hazdrová J, Skácelová K, Hájek J, Forbelská M (2015) Effect of dehydration on spectral reflectance and photosynthetic efficiency in *Umbilicaria arctica* and *U. hyperborea*. Biol Plant 59:357–365

Baruffo L, Piccotto M, Tretiach M (2008) Intrathalline variation of chlorophyll *a* fluorescence emission in the epiphytic lichen *Flavoparmelia caperata*. Bryologist 111(3):455–462

Bokhorst S, Tømmervik H, Callaghan TV, Phoenix GK, Bjerke JW (2012) Vegetation recovery following extreme winter warming events in the sub-Arctic estimated using NDVI from remote sensing and handheld passive proximal sensors. Environ Exp Bot 81:18–25

Büdel B, Scheidegger C (2008) Thallus morphology and anatomy. In: Nash TH (ed) Lichen biology. Cambrige University Press, Cambridge, pp 40–68

Butler MJ, Day AW (1998) Fungal melanins: a review. Can J Microbiol 44(12):1115–1136

Chekanov K, Feoktistov A, Lobakova E (2017) Spatial organization of the three-component lichen *Peltigera aphthosa* in functional terms. Physiol Plant 160:328–338

Chivkunova OB, Solovchenko AE, Sokolova SG, Merzlyak MN, Reshetnikova IV, Gitelson AA (2001) Reflectance spectral features and detection of superficial scald-induced browning in storing apple fruit. J Russ Phytopathol Soc 2:73–77

Conti S, Hazdrová J, Hájek J, Očenášová P, Barták M, Skácelová K, Adamo P (2014) Comparative analysis of heterogeneity of primary photosynthetic processes within fruticose lichen thalli: preliminary study of interspecific differences. Czech Polar Reports 4(2):149–157

Demmig-Adams B, Adams Iii WW (1992) Photoprotection and other responses of plants to high light stress. Annu Rev Plant Biol 43(1):599–626

Fortuna L, Baracchini E, Adami G, Tretiach M (2017) Melanization affects the content of selected elements in parmelioid lichens. J Chem Ecol 43(11):1086–1096

Gamon JA, Huemmrich KF, Stone RS, Tweedie CE (2013) Spatial and temporal variation in primary productivity (NDVI) of coastal Alaskan tundra: decreased vegetation growth following earlier snowmelt. Remote Sens Environ 129:144–153

Garty J, Weissman L, Tamir O, Beer S, Cohen Y, Karnieli A, Orlovsky L (2000) Comparison of five physiological parameters to assess the vitality of the lichen *Ramalina lacera* exposed to air pollution. Physiol Plant 109(4):410–418

Gauslaa Y, Solhaug KA (2001) Fungal melanins as a sun screen for symbiotic green algae in the lichen *Lobaria pulmonaria*. Oecologia 126(4):462–471

Gessler NN, Egorova AS, Belozerskaya TA (2014) Melanin pigments of fungi under extreme environmental conditions. Appl Biochem Microbiol 50(2):105–113

Gloser J, Gloser V (2007) Changes in spectral reflectance of a foliar lichen *Umbilicaria hirsuta* during desiccation. Biol Plant 51(2):395–398

Goltsev VN, Kalaji HM, Paunov M, Bąba W, Horaczek T, Mojski J, Kociel H, Allakhverdiev SI (2016) Variable chlorophyll fluorescence and its use for assessing physiological condition of plant photosynthetic apparatus. Russ J Plant Physiol 63(6):869–893

Hájek J, Barták M, Dubová J (2006) Inhibition of photosynthetic processes in foliose lichens induced by temperature and osmotic stress. Biol Plant 50(4):624–634

Hájek J, Barták M, Hazdrová J, Forbelská M (2016) Sensitivity of photosynthetic processes to freezing temperature in extremophilic lichens evaluated by linear cooling and chlorophyll fluorescence. Cryobiology 73(3):329–334

Honegger R (2008) Morphogenesis. In: Nash TH (ed) Lichen biology. Cambridge University Press, Cambridge, pp 69–93

Honegger R (2012) The symbiotic phenotype of lichen-forming ascomycetes and their endo- and epibionts. In: Hock B (ed) Fungal associations, the mycota IX, 2nd edn. Springer, Berlin, pp 287–339

Jensen M, Siebke K (1997) Technical report. fluorescence imaging of lichens in the macro scale. Symbiosis 23:183–196

Kalaji HM, Schansker G, Ladle RJ, Goltsev V, Bosa K, Allakhverdiev SI et al (2014) Frequently asked questions about in vivo chlorophyll fluorescence: practical issues. Photosynth Res 122(2):121–158

Kalaji HM, Jajoo A, Oukarroum A et al (2016) Chlorophyll *a* fluorescence as a tool to monitor physiological status of plants under abiotic stress conditions. Acta Physiol Plant 38(4):102

Kuusinen N, Juola J, Karki B, Stenroos S, Rautiainen M (2020) A spectral analysis of common boreal ground lichen species. Remote Sens Environ 247:111955

Lange OL, Green TA, Reichenberger H (1999) The response of lichen photosynthesis to external CO_2 concentration and its interaction with thallus water-status. J Plant Physiol 154(2):157–166

Lange OL, Green TA, Heber U (2001) Hydration-dependent photosynthetic production of lichens: what do laboratory studies tell us about field performance? J Exp Bot 52(363):2033–2042

Lange OL, Green TA, Melzer B, Meyer A, Zellner H (2006) Water relations and CO_2 exchange of the terrestrial lichen *Teloschistes capensis* in the Namib fog desert: measurements during two seasons in the field and under controlled conditions. Flora-Morphol Distrib Funct Ecol Plants 201(4):268–280

Lazár D (2006) The polyphasic chlorophyll *a* fluorescence rise measured under high intensity of exciting light. Funct Plant Biol 33:9–30

Lazár D (2015) Parameters of photosynthetic energy partitioning. J Plant Physiol 175:131–147

Mafole T (2017) Melanisation of lichens: the composition of melanin and the role of ultraviolet light (uv) in peltigeralean and non-peltigeralean Lichens (Doctoral dissertation)

Mafole TC, Chiang C, Solhaug KA, Beckett RP (2017) Melanisation in the old forest lichen *Lobaria pulmonaria* reduces the efficiency of photosynthesis. Fungal Ecol 29:103–110

Mafole TC, Solhaug KA, Minibayeva FV, Beckett RP (2019a) Tolerance to photoinhibition within a lichen species is higher in melanised thalli. Photosynthetica 57(1):96–102

Mafole TC, Solhaug KA, Minibayeva FV, Beckett RP (2019b) Occurrence and possible roles of melanic pigments in lichenized ascomycetes. Fungal Biol Rev 33(3–4):159–165

Maksimov EG, Schmitt FJ, Tsoraev GV, Ryabova AV, Friedrich T, Paschenko VZ (2014) Fluorescence quenching in the lichen *Peltigera aphthosa* due to desiccation. Plant Physiol Biochem 81:67–73

Matee LP, Beckett RP, Solhaug KA, Minibayeva FV (2016) Characterization and role of tyrosinases in the lichen *Lobaria pulmonaria* (L.) Hoffm. Lichenologist 48(4):311–322

McEvoy M, Gauslaa Y, Solhaug KA (2007a) Changes in pools of depsidones and melanins, and their function, during growth and acclimation under contrasting natural light in the lichen *Lobaria pulmonaria*. New Phytol 175(2):271–282

McEvoy M, Solhaug KA, Gauslaa Y (2007b) Solar radiation screening in usnic acid-containing cortices of the lichen *Nephroma arcticum*. Symbiosis 43:143–150

McLean J, Purvis OW, Williamson BJ, Bailey EH (1998) Role for lichen melanins in uranium remediation. Nature 391(6668):649

Palharini KMZ, Vitorino LC, Menino GCDO, Bessa LA (2020) Edge effects reflect the impact of the agricultural matrix on the corticolous lichens found in fragments of Cerrado Savanna in Central Brazil. Sustainability 12(17):7149

Parr CS, Wilson MN et al (2014) The encyclopedia of life v2: providing global access to knowledge about life on earth. Biodivers Data J 2:e1079

Peñuelas J, Filella I (1998) Visible and near-infrared reflectance techniques for diagnosing plant physiological status. Trends Plant Sci 3(4):151–156

Plonka PM, Grabacka M (2006) Melanin synthesis in microorganisms – biotechnological and medical aspects. Acta Biochim Pol 53:429443. https://doi.org/10.18388/abp.2006_3314

Rao DN, LeBlanc F (1965) A possible role of atranorin in the lichen thallus. Bryologist 68(3):284–289

Rassabina AE, Gurjanov OP, Beckett RP, Minibayeva FV (2020) Melanin from the Lichens *Cetraria islandica* and *Pseudevernia furfuracea*: structural features and physicochemical properties. Biochem Mosc 85:623–628

Raynolds MK, Walker DA, Verbyla D, Munger CA (2013) Patterns of change within a tundra landscape: 22-year Landsat NDVI trends in an area of the northern foothills of the Brooks Range, Alaska. Arct Antarct Alp Res 45(2):249–260

Rikkinen J (2015) Cyanolichens. Biodivers Conserv 24(4):973–993

Solhaug KA, Larsson P, Gauslaa Y (2010) Light screening in lichen cortices can be quantified by chlorophyll fluorescence techniques for both reflecting and absorbing pigments. Planta 231(5):1003–1011

Sotille ME, Bremer UF, Vieira G, Velho LF, Petsch C, Simões JC (2020) Evaluation of UAV and satellite-derived NDVI to map maritime Antarctic vegetation. Appl Geogr 125:102322

Stirbet A, Riznichenko GY, RubinGovindjee AB (2014) Modeling chlorophyll *a* fluorescence transient: relation to photosynthesis. Biochem Mosc 79(4):291–323

Stocker-Wörgötter E (2001) Experimental lichenology and microbiology of lichens: culture experiments, secondary chemistry of cultured mycobionts, resynthesis, and thallus morphogenesis. Bryologist 104(4):576–581

Strasser RJ, Stirbet AD (2001) Estimation of the energetic connectivity of PS II centres in plants using the fluorescence rise O–J–I–P: Fitting of experimental data to three different PS II models. Math Comput Simul 56(4):451–462

Strasser RJ, Tsimilli-Michael M, Srivastava A (2004) Analysis of the chlorophyll *a* fluorescence transient. In: Papageorgiou GC, Govindjee (eds) Chlorophyll a Fluorescence. Springer, Dordrecht, pp 321–362

Thomson JW (1972) Distribution patterns of American Arctic lichens. Can J Bot 50(5):1135–1156

Urbanavichyus GP (2011) Specific features of lichen diversity of Russia. Izvestiya Rossiiskoi Akademii Nauk Series Geography 1:66–87

Valladares F, Sancho LG, Ascaso C (1996) Functional analysis of the intrathalline and intracellular chlorophyll concentrations in the lichen family Umbilicariaceae. Ann Bot 78(4):471–477

Wu L, Zhang G, Lan S, Zhang D, Hu C (2014) Longitudinal photosynthetic gradient in crust lichens' thalli. Microb Ecol 67(4):888–896